

Dye-concentration-dependent lasing behaviors and spectral characteristics of cholesteric liquid crystals

Zhongyang Wang · Can Yang · Wensong Li ·
Lujian Chen · Xiaozhong Wang · Zhiping Cai

Received: 22 January 2013 / Accepted: 21 August 2013 / Published online: 8 September 2013
© Springer-Verlag Berlin Heidelberg 2013

Abstract The laser behavior and spectral changes occurring in cholesteric liquid crystals with varying dye-doped concentrations were investigated when pumped at 532 nm. It was found that the long-wavelength band edge and the laser line exhibit a blue shift over 21 nm with increasing dye concentration. The circularly polarized fluorescence spectra were examined, and the location of the sense reversion of circular polarization was determined to coincide well with the discrete lasing lines. The blue shift can be ascribed to the decrease in average refractive index and pitch of the dye-doped cholesteric liquid crystals. The dependence of the slope efficiency and threshold energy on the dye concentration can be attributed to the shift in photonic stopband and the change in penetration depth of excitation. The temperature and incident angle of pumping beam also have a significant impact on the lasing properties. The optimal dye concentration is found to be 0.5 wt% at 30.5 °C with an incident angle of 10°. The laser emission located at 601.4 nm with slope efficiency of 4 % was achieved above the threshold energy of 14.3 μ J.

1 Introduction

Inspired by the prospects for building compact, mirror-less and spectrally tunable laser devices, cholesteric liquid crystals (CLCs) attracted a growing interest during the past

decade since the first unequivocal observations of band-edge lasing in DDCLC [1–4]. Due to the anisotropic nature and a helical rotation of the local optical axis in CLCs, a one-dimensional photonic band gap (PBG) similar to a conventional Bragg stack is established. However, the stopband condition only holds for the circularly polarized (CP) light with the same rotation sense as the helix. When the CLC is doped with a fluorescence dye and the spontaneous emission of photons is suppressed within the gap and sharply enhanced at the long- and short-wavelength edges of the PBG, the fluorescence photons have a very slow group velocity and a very large density of photonic states (DOS) at both band edges [2, 3]. Then, laser outputs are possibly achieved through optical pumping, when the emission enhancement at the band edges is sufficient to enable low-threshold laser actions.

Generally, the long-wavelength band edge has been proven to favor lasing emissions with the lowest threshold mode, because of the collinearity of the transition dipole moment of the dye and the electric field vector [2]. For a traditional down-conversion fluorescence lasing excitation, a shorter excitation wavelength defined by the wavelength dependence of the dye absorption is used to induce an electronic transition to the first excited state, e.g., S_0 – S_1 . Due to the high birefringence required to correlate with low thresholds and high slope efficiencies, the PBG of the selected CLCs is usually broad, and therefore, it might overlap with the excitation wavelength, thus reducing the pumping efficiency [4]. An increased pumping efficiency can be achieved by carefully keeping the wavelength of excitation beam away from the PBG or converting its polarization to an opposite sense of rotation of the helix and would thus minimize the impact of the laser lines.

The primary concern in the development of DDCLC lasers toward practical applications is the strategies with

Z. Wang · C. Yang · W. Li · L. Chen (✉) · X. Wang (✉) ·
Z. Cai
Department of Electronic Engineering, Xiamen University,
Xiamen 361005, People's Republic of China
e-mail: lujianchen@xmu.edu.cn

X. Wang
e-mail: wangxz@xmu.edu.cn

which to enhance the laser performance. Some interesting relationships between the lasing behavior and the form of the material properties such as birefringence, order parameter, and the cell design have been investigated [4–7]. In addition to the input–output characteristics, the spectral tunability can readily be realized by means of temperature changes of the helical pitch, p [5]. Other complicated methods like changing the species and concentration of the chiral dopant, using wedge cells, and applying external stimuli, including light illumination and electric field, etc., were employed to control the helical pitch [8–16].

The motivation of this study is to optimize the materials from which the devices are constructed by a quantitative investigation of the threshold and the slope efficiency of the DDCLC lasers under different conditions, e.g., the dye concentration, incident angle of the pump beam, and temperature. We experimentally demonstrated here the possibility of tuning the laser emission wavelength over 21 nm at varying dye concentrations and discussed the relevance of the refractive index, pitch, and CP fluorescence spectra to the blue shift of lasing lines.

2 Experimental

The CLC samples were prepared by mixing a nematic liquid crystal E7 (Merck) and a left-handed (LH) chiral dopant S811 (Merck), with a weight percentage of 0.73:0.27. The concentrations of laser dye pyromethene 597 (PM597, Exciton) in CLC were 0.1, 0.3, 0.5, 0.7, 0.9, 1.0, and 1.5 wt%, respectively. We measured the refractive indices of nematic E7 with different dye concentrations of 0, 0.1, 0.3, and 0.5 wt% using an Abbe refractometer (Atago DR-M4) at $\lambda = 589$ nm. The temperature of the Abbe refractometer is controlled by a circulating constant temperature bath and maintained at 30.5 °C.

The DDCLCs were mixed ultrasonically and heated in the oven to ensure a full dissolution and uniformity. Then they were injected into the empty cells using the capillary effect to form a planar texture. The empty cell was pre-fabricated by combining two indium-tin-oxide-coated glass slides separated by 18- μm -thick plastic spacers (cell gap). Both glass slides in each cell were pre-coated with polyimide film and pre-rubbed in the same direction to favor a homogeneous alignment. To determine p , glass slides were assembled to form a wedge cell with an opening angle α , and the classical Grandjean–Cano wedge method was used [17].

Figure 1 shows the schematic diagram of the experimental setup for measuring the lasing and fluorescence spectra in the visible region at various incident angles. The samples were mounted on a temperature-controlled heating stage. For the measurement of band-edge laser emission, a

Q-switched Nd:YAG second harmonic pulsed laser ($\lambda = 532$ nm) with pulse duration of 12 ns and repetition frequency of 1 Hz was modulated by a pair of Glan–Taylor prisms and transformed into a CP light by a quarter waveplate to excite the DDCLC sample. Thus, the CP incident light with opposite sense of rotation of the helix would minimize the impact on the band gap. A lens ($f = 100$ mm) was used to focus the pumping beam, and the diameter of the focused spot was about 100 μm . The pump beam was obliquely incident on the mounted sample on a rotating stage at an angle α ($\alpha = 10^\circ$ if not specially mentioned) with respect to the normal of the cell plate. For the measurement of fluorescence emission, the pulsed laser was replaced by a 5-mw continuous-wave (cw) Nd:YAG laser ($\lambda = 532$ nm).

The emitted light was collected by another lens ($f = 100$ mm) along the cell normal parallel to the helix axis in the forward direction, then directed through a long-pass filter (>550 nm) toward a fiber-optic bundle connected to a fiber spectrometer (HR2000+, Ocean Optics) with a spectral resolution less than 0.5 nm. Whereas the fluorescence spectra were measured using another fiber spectrometer (EPP2000, StellarNet) with a resolution of about 2 nm, the reflection spectra were recorded by a Lambda 750 UV/Vis/NIR spectrophotometer from Perkin-Elmer.

In order to further quantify the CP properties, an achromatic quarter waveplate followed by a linear polarizer was inserted in the optical path between the collecting lens and the spectrometer to act as a circular analyzer. The achromatic quarter helps to translate the CP emission into linearly polarized light. By rotating the linear polarizer in front of the spectrometer to change its orientation with respect to the optical axis of the waveplate, the polarization state of the light emission from the samples can be checked. To study the slope efficiency of the lasers, the input and output energies were monitored using a PE10

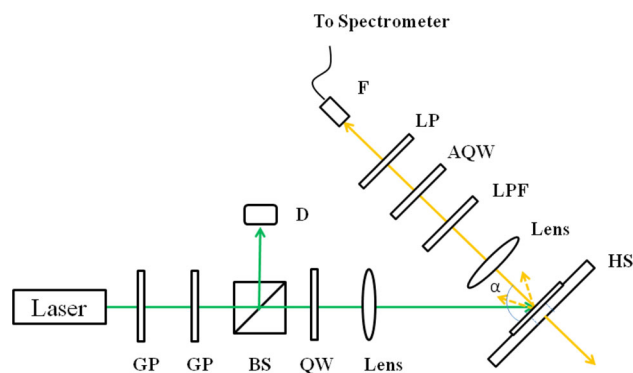


Fig. 1 Schematic diagram of the experimental setup: GP Glan–Taylor prism, BS beam splitter, D detector, QW quarter waveplate, HS hot stage, LPF long-pass filter, AQW achromatic quarter waveplate, LP linear polarizer, F fiber connected to spectrometer

pyroelectric detector and a PD10 silicon photodiode detector with energy meters (Nova, Ophir). The emission energies are doubled to take into account the emission from both sides.

3 Results and discussion

The nematic liquid crystal E7 is miscible with the chiral dopant S811 over their entire concentration range. The binary E7/S811 mixture with weight percentage of 0.73:0.27 forms the CLC phase in the temperature range (29.5–32.5 °C) studied here, when slowly cooled from the isotropic phase [18]. As shown in Fig. 2a, a narrow-line-width laser operation with tuning wavelength of about 21 nm is achieved by the addition of laser dye. The addition of relatively large dye molecules would influence the order parameter of the mixture. Since birefringence decreases, the width of the band also decreases. This also explains the narrowing of the selective reflection band. The unpolarized fluorescence has been normalized for comparison as depicted in Fig. 2b. With the low-energy excitation from the cw Nd:YAG laser, the spectrum is dominated by a broad spontaneous emission. And the suppression of the emission inside the PBG was evidenced by the shoulder next to the gain maximum, which can be attributed to the light enhancement at the band edge.

We monitored the relative spectral intensity of the discrete lasing line to investigate the polarization dependence using the experimental setup described above. As the linear polarizer is rotated gradually, the relative intensity detected by the spectrometer as shown in Fig. 3a is dependent upon rotation angle. The curve with triangle symbols depicts the intensities that were recorded using the combination of achromatic quarter waveplate and linear polarizer. When the linear polarizer is oriented at $+45^\circ/-45^\circ$ to the optical axis of the achromatic quarter waveplate, only the pure single-handed circular luminescence can be fully translated into linear polarized state. While the achromatic quarter waveplate is removed, approximately equal intensities through the rotating linear polarizer are detected as depicted by the curve with circle symbols. The shape of two curves in the polar coordinate confirms a LH CP laser emission [20]. Figure 3b depicts the intensity variation in the LH CP laser emission with the incident pump energy for a traditional sample with dye concentration of 0.5 wt%. A kink in the curve signifying the threshold is observed. The lasing emission grows linearly with excitation above the input energy of 14.3 μJ , indicating a distinct lasing behavior [19]. The straight line that fits the data is used to determine the slope efficiency. The overall loss caused by the optical collecting elements is not taken into account when calculating the slope efficiency.

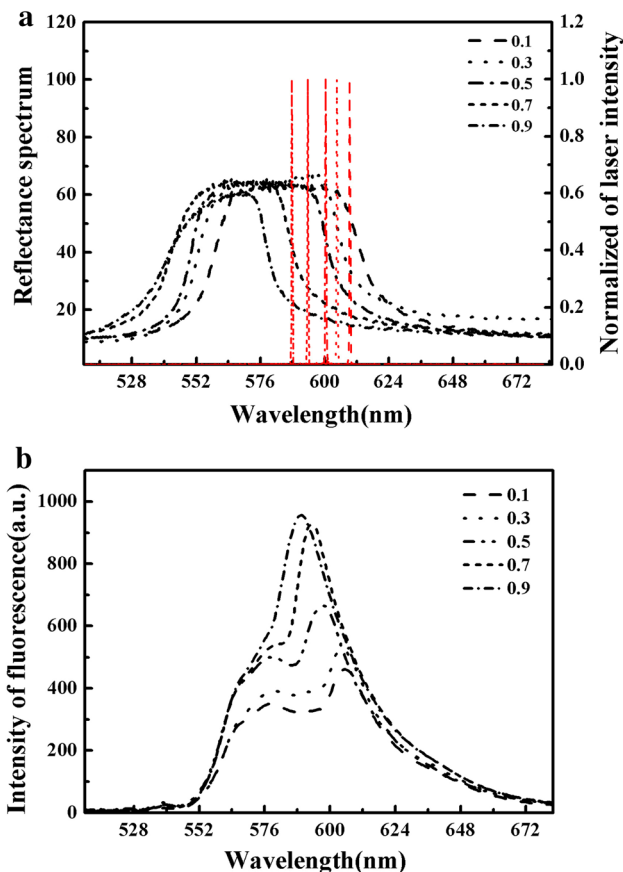


Fig. 2 Spectral characteristics for a typical DDCLC sample viewed under normal angle with dye concentration of 0.5 wt% at 30.5 °C. **a** The reflection spectra show the long-wavelength band edge (primary y-axis). The normalized emission spectra show the band-edge laser (secondary y-axis). **b** The un-polarized fluorescence emission with different dye concentrations

When no dye is doped, the CLC host exhibits a PBG from 580 to 630 nm, covering a wavelength range of about 50 nm. The stopband shifts to short wavelength as the dye concentration increases simultaneously, in accordance with the blue shift of the laser emission. It should be also noted that the shifts are discontinuous, which is very similar to what we found with the temperature change as summarized in Table 1, in a stepwise manner, so as to ensure that a one half-integer number of turns fit between the boundaries [21]. For a CLC cell composed of two parallel glass plates with a cell gap d , the discrete spectral values separated by the free spectral range $\Delta\lambda$ can be calculated by Funamoto et al. [22] as follows:

$$\frac{nd}{\lambda + \Delta\lambda} = \frac{nd}{\lambda} - \frac{1}{2} \quad (1)$$

with $d = 18 \mu\text{m}$ and the average index $n = 1.68$, which can be calculated by the function $n = \sqrt{(n_o^2 + 2n_e^2)}/3$, where $n_o = 1.52$, $n_e = 1.75$. And the approximate laser wavelength $\lambda = 600 \text{ nm}$ for the CLC cell is taken into

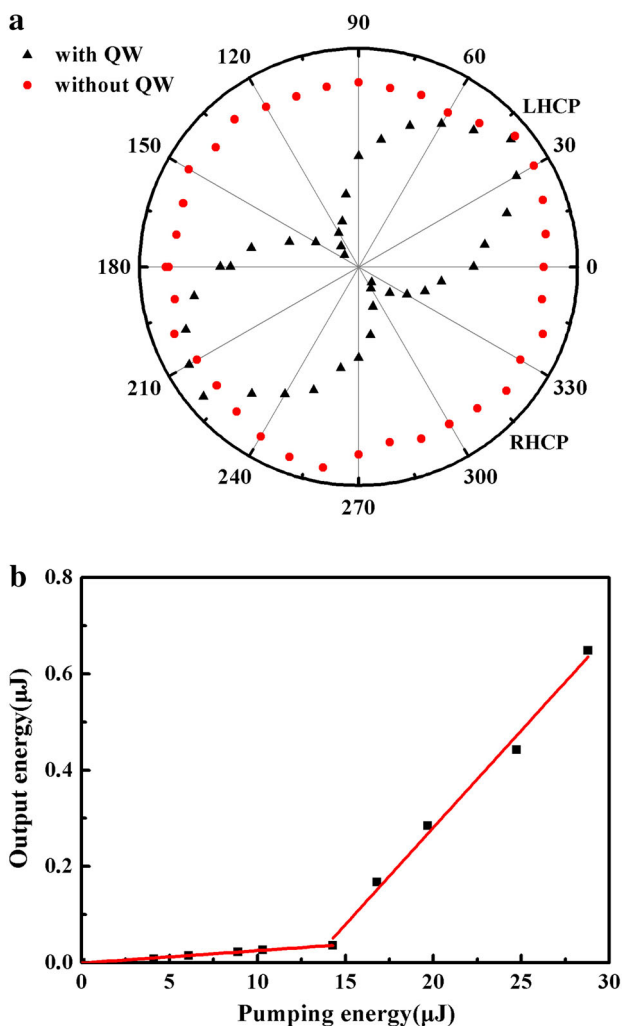


Fig. 3 **a** Polar plots of the lasing output intensity versus the azimuthal angle of the linear polarizer for a typical DDCLC sample by inserting the achromatic quarter waveplate (*circle symbols*) and not inserting the achromatic quarter waveplate (*triangle symbols*). **b** The total emission intensity from both sides as a function of excitation energy for a typical DDCLC sample with dye concentration of 0.5 wt% at 30.5 °C

account here. The wavelength difference between adjacent laser lines ($\Delta\lambda$) is estimated to be 6.1 nm, which is close to the average experimental value of 5.6 nm.

Belyakov has already proved that there exists an optimum angle for pumping theoretically, at which the threshold significantly reduces [23]. Here, we experimentally studied the influence of operating temperature on threshold energy and slope efficiency as summarized in Table 1. With the increase in operating temperature, the threshold increases gradually. But the slope efficiency reaches the largest value at 30.5 °C, corresponding to the gain maximum of PM597 dye as shown in Fig. 2b. The increased order parameter relating to the DDCLCs at lower temperature was considered to be a principle factor that is responsible for the increased performance [5]. As depicted

in Table 2, the percentage of totally absorbed energy decreases with the increase in incident angle, leading to the deprivation of laser performance. The lowest threshold and the highest slope efficiency can be achieved with the incident angle of 10°. This measured value is close to the calculated one of 17.1° using the expression derived in Belyakov’s work [23], relating the optimum pump angle to the laser wavelength. The difference between the two values might be attributed to the impact of temperature on the dielectric constant and other uncertainties.

Although a RH CP incident light with opposite sense of rotation of the CLC helix was adopted in our study to overcome the unexpected PBG reflection, we still recorded that over 30 % pumping energy was transmitted and reflected at an incident angle of 10°. Therefore, the efficiencies obtained in the current binary E7/S811 mixture are smaller than other CLCs where PM597 was also used to provide gain profile [5, 24]. We suspect that the feedback is also provided by the waveguide formed by the liquid crystal and the two glasses in the manner of the competitive quasi-in-plane leaky (QIPL) modes. The leaking light energy out of the cell within the glasses at a grazing angle might dramatically reduce the band-edge lasing efficiency we are concerned with [25].

In the unpolarized fluorescence shown previously in Fig. 2b, two distinguishable peaks can be found in most of the samples. The two peaks merge into one with the increase in the dye concentration finally. The somewhat

Table 1 Laser properties of the DDCLC operated at different temperatures when doped with 0.5 wt% dye concentrations with an incident excitation angle of 10°

Temperature (°C)	Laser wavelength (nm)	Slope efficiency (%)	Threshold (μJ)
29.5	611.2	3.0	12.7
30.0	606.5	3.6	13.3
30.5	601.4	4.0	14.3
31.0	598.3	3.3	16.2
31.5	593.4	2.0	17.2
32.0	589.2	1.9	18.0
32.5	584.0	1.8	18.4

Table 2 Laser properties of the DDCLC operated with different incident excitation angles at 30.5 °C when doped with 0.5 wt% dye concentration

Incident angle (°)	Slope efficiency (%)	Threshold (μJ)
10.0	4.0	14.3
20.0	3.4	15.2
30.0	2.4	17.3
40.0	2.0	18.5

ambiguous spectral changes in the corresponding emission peak at the long-wavelength region by varying dye concentrations are obscure because of the overlap of emissions with different handedness. In order to have a better insight into the phenomenon, the characteristics and analyses of the CP fluorescence are necessary [26, 27]. The CP fluorescence spectra were examined to distinguish the emissions with both left-handed (LH) and right-handed (RH) circular polarizations, presented in Fig. 4a, b, respectively. After transmitting through the well-oriented quarter waveplate, the CP light turns into linear polarized light. It should be noted that only one maximum is found from the samples with low dye concentrations (0.1 and 0.3 wt%) in the RH spectra. It is similar to that measured in an isotropic solvent, differing from the situation in the unpolarized fluorescence (Fig. 2b). The LH emission in DDCLCs with an equal sense of chirality is suppressed within the PBG and enhanced at the band edge, as a consequence of the optical dispersion relation [26].

The sense reversion of CP at the edges of the PBG provides a tool to exploit the DOS divergence, which is connected with the band-edge lasing behavior. A practical way is to quantify the degree of CP by $g(\lambda)$, which is defined by Voigt et al. [26],

$$g(\lambda) = 2 \frac{I_L(\lambda) - I_R(\lambda)}{I_L(\lambda) + I_R(\lambda)} = 2 \frac{r(\lambda) - 1}{r(\lambda) + 1}, \quad (2)$$

with $I_L(\lambda)$ and $I_R(\lambda)$ as intensity of left/right-hand CP light intensity, and r as left/right-handed intensity ratio. $g(\lambda) = +2/-2$ Corresponds to completely left/right-handed CP luminescence, whereas unpolarized luminescence has $g(\lambda) = 0$.

Figure 4c shows the degree of $g(\lambda)$ calculated using the Eq. (2), from the data of CP fluorescence spectra in Fig. 4a, b. The $g(\lambda)$ value can be used to quantify the polarization states for CP fluorescence, which is connected to the formation of band gap [26]. It shows that the maximum of $g(\lambda)$ value decreases with increasing dye concentration, much lower than the ideal maximum value of 2. As we know, a minimum number of CLC pitch periods are necessary to establish a well-developed band gap for laser [3]. Higher dye concentration also leads to shorter penetration depth of the excitation. Only dyes in a thin layer close to the surface can contribute to the emission behavior. Thus, the dyes do not experience a well-developed band gap and can still emit light with different polarization states. So the observed $g(\lambda)$ is reduced with the increase in dye concentration. Meanwhile, the increase in dye concentration facilitates the blue shift of the location of sign reversal in $g(\lambda)$ at long-wavelength edge. The sign reversal is pegged to the DDCLC band edge, corresponding to a shorter helical pitch of CLC [26]. The short-wavelength band edge

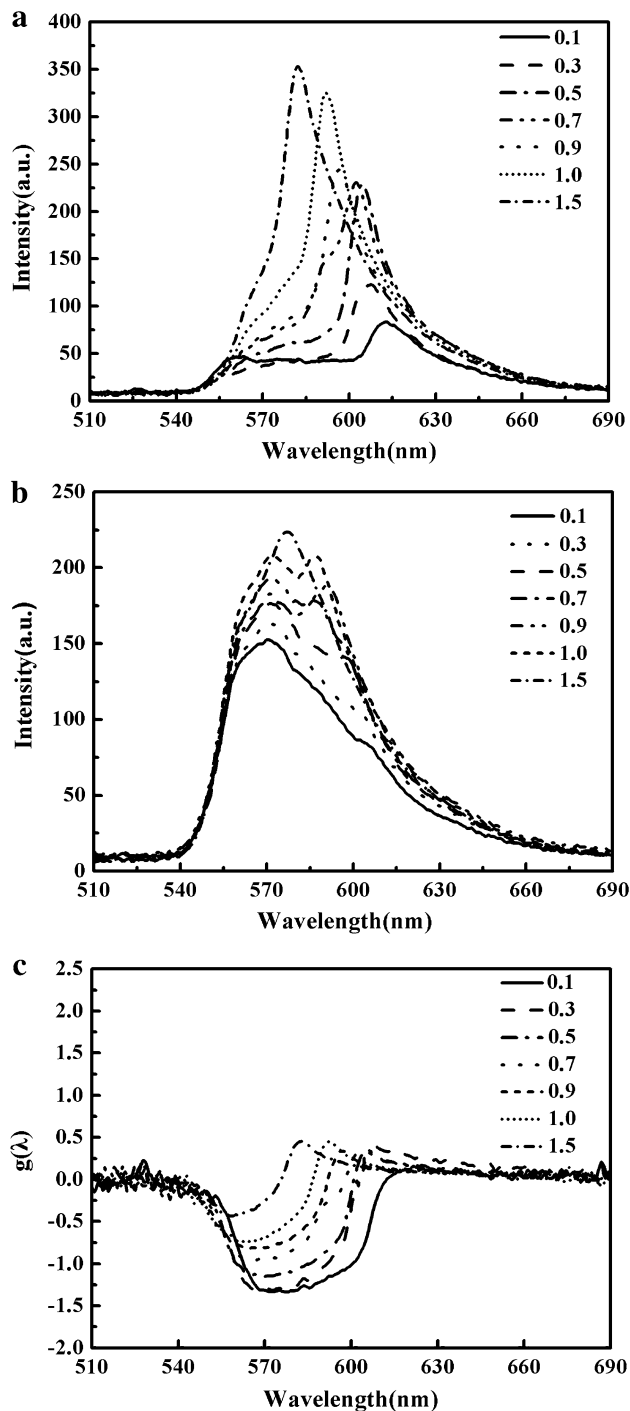


Fig. 4 LH CP (a), RH CP (b) fluorescence emission spectra and (c) $g(\lambda)$ calculated from the polarization ratio of LH/RH emissions according to Eq. (2)

is not observed because it is outside the fluorescence wavelength.

To evaluate the location of stopband and the lasing wavelength, we need to know the refractive index and the pitch of the DDCLC. But it is difficult to get the refractive indices of the CLC samples directly using commercially

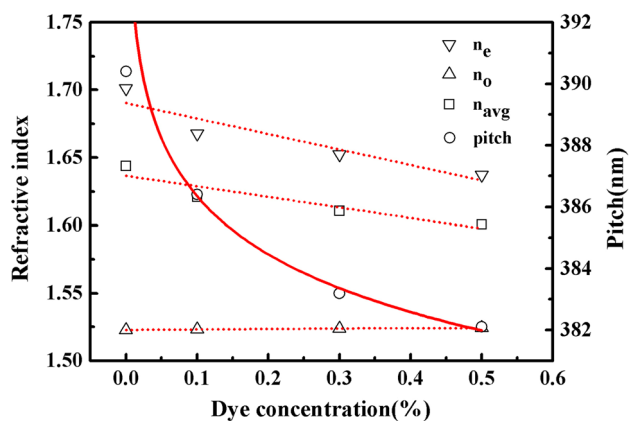


Fig. 5 Dye-concentration-dependent **a** refractive indices of nematic liquid crystal E7 at 589 nm measured at 30.5 °C. *Upward triangles, downward triangles and squares* are the ordinary (n_o), extraordinary (n_e), and average refractive indices (n_{avg}), respectively (primary y-axis), **b** pitch estimated in the Grandjean–Cano wedge experiment, represented by *open circles* (secondary y-axis). The *dashed lines* are to direct the eye

available instruments like Abbe refractometer. Instead, we measured the refractive indices of the dye-doped nematic samples. No result from the E7 liquid crystals with higher doping concentrations was obtained due to the strong absorption at 589 nm, which were selected to coincide with lasing wavelengths. Figure 5 depicts refractive indices with dye concentrations of 0, 0.1, 0.3, and 0.5 wt%. Upward triangles, downward triangles and squares are the experimental data of ordinary (n_o), extraordinary (n_e), and average refractive indices (n_{avg}), respectively. When the dye concentration is increased, n_e significantly decreases and n_o slightly increases. The overall average index decreases. Furthermore, we calculated the value of p from the distance L between the disclination lines and α using the equation $p \approx 2L\alpha$ in the Grandjean–Cano wedge experiment and averaged over many measurements to reduce the errors. As represented by open circles in Fig. 5, the value of pitch decreases when the dye concentration increases. Assuming that the introduction of chiral dopant only helps to build up the helix axis, but does not influence this downtrend of refractive indices, we can predict that the stopband in the DDCLC should move to shorter wavelength when

p decreases. Summarizing, the blue shift of band edge and lasing wavelength can be ascribed to the decrease in average refractive index and the pitch.

Although increasing the dye concentration is supposed to help enhance the gain to a certain extent, it is implied that there should be a compromise between the gain-enhancing, band-gap-forming, and laser performance. The influence of the dye concentration on the location of sign reversal in $g(\lambda)$, laser wavelength, slope efficiency, and threshold energy was quantitatively summarized in Table 3. In these cases, the focused beam was incident obliquely on the sample with an incident angle of 10° at 30.5 °C. The location of sign reversal in $g(\lambda)$ coincides well with the laser wavelengths and also the wavelength spacing between adjacent laser lines calculated using Eq. (1). The linearly increased threshold can be ascribed to two main factors: fewer experienced CLC pitch periods induced by the shorter penetration depth of excitation beam in highly dye-doped samples and the relative position of the long-wavelength edge mode with respect to that of the gain maximum changed by the blue shift of the band gap as depicted in Fig. 2. It is also consistent with the vanished lasing behavior in the 1.5 wt% sample as discussed above. An optimum slope efficiency of 4.0 % can be realized in the 0.5 wt% sample.

4 Conclusions

In conclusion, we prepared DDCLCs with the E7/S811 mixture doped with different amounts of PM597 dye. The match of long-wavelength band edge provided by the CLCs and the gain profile of the dye supports a LH CP laser with a tunable range over 21 nm by adjusting the dye concentration. The CP fluorescence spectra were examined to measure the degree of the CP sense reversion at the edges of the PBG, which shows a coincidence with the discontinuous blue shift of the laser wavelength. The blue shift can be ascribed to the decrease in average refractive index and pitch of the DDCLC. The location of photonic stopband with respect to the gain maximum and the penetration depth of excitation are supposed to play an important role on the slope efficiency and threshold energy.

Table 3 Laser properties of the DDCLCs doped with different dye concentrations operated at 30.5 °C with an incident excitation angle of 10°

Dye concentration (wt%)	Location of sign reversal in $g(\lambda)$	Laser wavelength (nm)	Threshold (μJ)	Slope efficiency (%)
0.1	610	610.6	8.9	0.6
0.3	605	605.8	11.0	0.8
0.5	600	601.4	14.3	4.0
0.7	594.4	595.1	15.1	2.9
0.9	588	589.3	16.2	1.8

The best slope efficiency of 4 % was acquired with the 0.5 wt% sample above threshold energy of 14.3 μJ , when operated at 30.5 °C with an incident angle of 10°.

Acknowledgments This work was financially support by the National Natural Science Foundation of China under Grant 50802080 and the Natural Science Foundation of Fujian Province, China, under Grant 2010J01349.

References

1. V.I. Kopp, B. Fan, H.K.M. Vithana, A.Z. Genack, *Opt. Lett.* **23**, 1707 (1998)
2. G.E. Nevskaya, S.P. Palto, M.G. Tomilin, *J. Opt. Technol.* **77**, 473 (2010)
3. H. Coles, S. Morris, *Nat. Photonics* **4**, 676 (2010)
4. S.M. Morris, A.D. Ford, C. Gillespie, M.N. Pivnenko, O. Hadeler, H.J. Coles, *J. Soc. Inf. Display.* **14**, 565 (2006)
5. S.M. Morris, A.D. Ford, M.N. Pivnenko, H.J. Coles, *J. Appl. Phys.* **97**, 023103 (2005)
6. S. Morris, A. Ford, M. Pivnenko, O. Hadeler, H. Coles, *Phys. Rev. E* **4**, 061709 (2006)
7. Y. Inoue, H. Yoshida, K. Inoue, A. Fujii, M. Ozaki, *Appl. Phys. Express* **3**, 102702 (2010)
8. Y.G.F. Andy, L.T. Hsien, J.H. Liu, F.C. Wu, *Opt. Express* **12**, 1857 (2004)
9. M.Y. Jeong, J.W. Wu, *Opt. Express* **23**, 24221 (2010)
10. J.R. Schmidtke, G. Jünnemann, S.K. Baumann, H.S. Kitzerow, *Appl. Phys. Lett.* **101**, 051117 (2012)
11. M.Y. Jeong, H. Choi, J.W. Wu, *Appl. Phys. Lett.* **92**, 051108 (2008)
12. T.H. Lin, Y.J. Chen, C.H. Wu, A.Y.G. Fuh, J.H. Liu, P.C. Yang, *Appl. Phys. Lett.* **86**, 161120 (2005)
13. S. Furumi, S. Yokoyama, A. Otomo, S. Mashiko, *Appl. Phys. Lett.* **84**, 2491 (2004)
14. G. Chilaya, A. Chanishvili, G. Petriashvili, R. Barberi, R. Bartolino, *Adv. Mater.* **19**, 265 (2006)
15. G. Chilaya, A. Chanishvili, G. Petriashvili, R. Barberi, R. Bartolino, G. Cipparrone, A. Mazzulla, P.V. Shibaev, *Adv. Mater.* **19**, 565 (2007)
16. P. Shibaev, R. Sanford, D. Chiappetta, V. Milner, A. Genack, A. Bobrovsky, *Opt. Express* **13**, 2363 (2005)
17. D. Podolskyy, O. Banji, P. Rudquist, *Liq. Cryst.* **35**, 791 (2008)
18. W.R. Chen, J.C.H. Wang, *Liq. Cryst.* **31**, 1539 (2004)
19. I.D.W. Samuel, E.B. Namdas, G.A. Turnbull, *Nat. Photonics* **3**, 546 (2009)
20. F. Chen, D. Gindre, J.M. Nunizi, *Opt. Express* **16**, 16746 (2008)
21. S.M. Morris, A.D. Ford, H.J. Coles, *J. Appl. Phys.* **106**, 023112 (2009)
22. K. Funamoto, M. Ozaki, K. Yoshino, *Jpn. J. Appl. Phys.* **42**, 1523 (2003)
23. V.A. Belyakov, S.V. Semenov, *J. Exp. Theor. Phys.* **109**, 699 (2009)
24. C. Mowatt, S.M. Morris, M.H. Song, T.D. Wilkinson, R.H. Friend, H.J. Coles, *J. Appl. Phys.* **107**, 043101 (2010)
25. L.M. Blinov, G. Cipparrone, A. Mazzulla, P. Pagliusi, V.V. Lazarev, *J. Appl. Phys.* **101**, 053104 (2007)
26. M. Voigt, M. Chambers, M. Grell, *Liq. Cryst.* **29**, 653 (2002)
27. M. Voigt, M. Chambers, M. Grell, *Chem. Phys. Lett.* **347**, 173 (2001)